

## MR Direct Thrombus Imaging with optimised signal and improved lipid suppression

Andrew Nicholas Priest<sup>1</sup>, Ilse Joubert<sup>1</sup>, Sarah Hilborne<sup>1</sup>, Sally Hunter<sup>1</sup>, David J Bowden<sup>1</sup>, Martin John Graves<sup>1</sup>, Trevor Baglin<sup>2</sup>, Jonathan H Gillard<sup>1</sup>, and David John Lomas<sup>1</sup>

<sup>1</sup>Department of Radiology, Addenbrookes Hospital and University of Cambridge, Cambridge, United Kingdom, <sup>2</sup>Department of Haematology, Addenbrookes Hospital, Cambridge, United Kingdom

**Target audience** Physicists and clinicians concerned with venous thrombo-embolism or atherosclerotic plaque thrombosis

### Purpose

MR Direct Thrombus Imaging (MR-DTI) is able to highlight acute thrombus, while suppressing signal from background tissues, due to the short T1 relaxation time of met-haemoglobin.<sup>1</sup> It can accurately detect deep vein thrombosis (DVT)<sup>2</sup> and may be particularly valuable in diagnosing acute recurrent DVT in a previously affected venous segment.<sup>3</sup> MR-DTI has also been used to identify carotid intraplaque haemorrhage,<sup>4</sup> a significant factor in the vulnerability of plaques to instability and rupture. In this study, simulations and phantom measurements are used to optimise the signal-to-noise ratio (SNR) of MR-DTI. Furthermore, traditional spectral fat suppression methods can fail near the edges of the field of view, which can interfere with thrombus detection. For improved fat suppression in these regions, we also investigate the combination of MR-DTI with Dixon imaging.

### Methods

The expected signal intensity of the MR-DTI sequence was simulated using Matlab (Mathworks, Natick, MA), assuming perfect spoiling within the fast gradient-echo readout. An adjustable delay ( $T_D$ ) was added between the end of the readout and the subsequent inversion pulse. Three parameters ( $T_D$ , inversion time  $T_I$ , flip angle  $\alpha$ ) were varied to find near-maximal values of the signal from short T1 tissues (e.g. thrombus) whilst approximately nulling the blood signal. The difference between simulated signals at the centre of k-space was compared, as was the variation across k-space (which affects the point-spread function). Comparisons were made for linear or centric ordering, for full or partial k-space acquisition, and for  $n=1$  or  $n=2$  (where  $n$  is the number of shots per k-space plane). The following acquisition parameters were assumed: TE 6.3 ms, TR 12.2 ms, matrix 320x288x96, FoV 40x40 cm<sup>2</sup>, slice thickness 2mm, ASSET factor 2, 2 discarded acquisitions after each inversion.

MR-DTI was implemented on a 1.5 T MR system (Discovery MR450, GE Healthcare, Waukesha, WI) using adiabatic inversion and spectral-spatial excitation during the readout. Measurements of SNR were made in a Eurospin T05 phantom using gels with T1 values (446 and 1246 ms) which were near to those expected for thrombus and blood.

Additionally, an alternative version of MR-DTI was implemented using dual echo Dixon imaging for fat suppression instead of the spatial-spectral excitation. The Dixon method allowed automated reconstruction of water-only and fat-only images from acquired in-phase and out-of-phase images (TE 2.1/4.3 ms, TR 6.6 ms).

Following ethical approval and informed consent, MR-DTI images were acquired from 2 patients with DVT, diagnosed by compression ultrasound, and one patient with carotid atheroma, suspected to have intraplaque haemorrhage. In one of the DVT patients both conventional and Dixon MR-DTI were acquired.

### Results

Fig. 1 shows simulations using near-optimal parameters for linear and centric encoding with  $n=1$  and  $n=2$ . In order to achieve blood suppression at the centre of k-space, partial Fourier was required for linear encoding but not for centric encoding. Linear encoding typically led to substantial signal variation across k-space, and images showed artifacts, probably because the homodyne reconstruction was disrupted by the signal reversal around k-space centre. In contrast, centric encoding was found to offer more uniform signal across k-space, including greater signal levels at the centre of k-space, and gave good quality phantom images. Increasing to  $n=2$  shots with centric ordering allowed increased flip angles to be used effectively, giving slightly higher signal and reduced variation across k-space compared with  $n=1$ .

Phantom images acquired with centric encoding (not shown) demonstrated high signal for short T1 and good suppression for 'blood' T1. Measured 'thrombus' SNR for linear, centric  $n=1$  and centric  $n=2$  were 29.5, 50.3, 56.8, while simulations of signal levels were 3.85, 6.69, 7.15 respectively; the relative levels of these signals are consistent, as expected, while 'blood' was suppressed in each case (measured SNR 2.9, 6.3, 8.3; simulated signal 0.12, 0.35, 0.51).

The best parameters with  $n=2$  (right-hand image in Fig. 1) were used for the patient study. The resulting images are shown in Fig. 2 for a patient with DVT. Fig. 3 shows coronal image from a patient with carotid plaque haemorrhage. Both cases are clearly depicted with good blood suppression.

Fig. 4 shows a comparison of the two versions of MR-DTI using spectral and Dixon methods for fat suppression. Both images depict the thrombus, but for the conventional version it is difficult to determine its superior and inferior extent due to failure of the fat suppression. For the Dixon version, fat suppression around the edge of the image is improved and the thrombus is depicted in these regions.

### Discussion

MR-DTI has the potential to become an important tool for diagnosis of acute thrombus, and the optimisations shown here may allow higher-resolution imaging. Fat suppression is particularly important in a method which highlights thrombus based on its short T1. Unlike spectral fat-suppression methods, Dixon imaging does not rely on obtaining a good shim, and is here applied (for the first time to our knowledge) to MR-DTI.

### Conclusion

Simulations have allowed the signal from MR-DTI to be optimised while suppressing the blood signal. Fat suppression may be improved by combining Dixon imaging with MR-DTI, instead of using chemical-shift-based methods, allowing better visualisation of thrombus near the edges of the image.

### References

1. Moody AR. Magnetic resonance direct thrombus imaging. *J Thromb Haemost.* 2003;1(7):1403-9.
2. Fraser DG, Moody AR, Morgan PS, et al. Diagnosis of lower-limb deep venous thrombosis: a prospective blinded study of magnetic resonance direct thrombus imaging. *Ann Intern Med.* 2002;136(2):89-98.
3. Westerbeek RE, Van Rooden CJ, Tan M, Van Gils AP, Kok S, De Bats MJ, De Roos A, Huisman MV. Magnetic resonance direct thrombus imaging of the evolution of acute deep vein thrombosis of the leg. *J Thromb Haemost.* 2008;6(7):1087-92.
4. Moody AR, Murphy RE, Morgan PS, et al. Characterization of complicated carotid plaque with magnetic resonance direct thrombus imaging in patients with cerebral ischemia. *Circulation.* 2003;107(24):3047-3052.

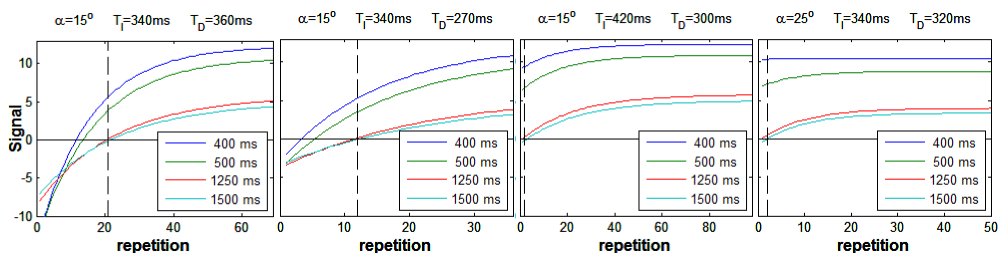


**Fig. 1: Simulated variation of signal through the readout train with (left to right) linear  $n=1$  and  $n=2$ , and centric  $n=1$  and  $n=2$ . The dashed line marks the centre of k-space.  $T_I$ ,  $T_D$  and  $\alpha$  are shown above each plot.**



**Fig. 2: Curved-plane reformat of MR-DTI, showing a large thrombus in the left femoral/popliteal vein, while blood (e.g. in the contralateral vein) is dark.**

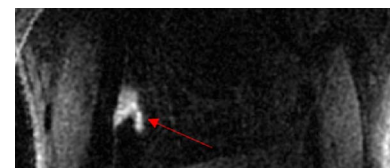


**Fig. 3: Carotid plaque haemorrhage.**

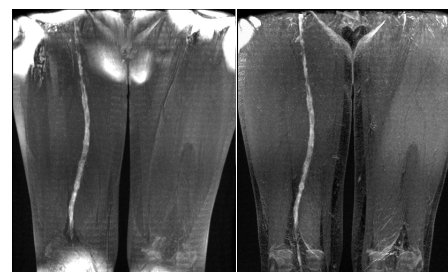


**Fig. 4: DVT in the right femoral/popliteal vein, viewed as thin-slab MIPs of conventional (left) and Dixon (right) versions of Direct Thrombus Imaging. Near the edges of the FOV, the overlying fat signal is greatly reduced for the Dixon technique.**